

Novel Vesicular Aggregates of Crown-Appended Cholesterol Derivatives Which Act as Gelators of Organic Solvents and as Templates for Silica Transcription

Jong Hwa Jung, Yoshiyuki Ono, Kazuo Sakurai, Masahito Sano, and Seiji Shinkai*

Contribution from the Chemotransfiguration Project, Japan Science and Technology Corporation (JST), 2432 Aikawa, Kurume, Fukuoka 839-0861, Japan

Received May 11, 2000

Abstract: New diazacrown-appended cholesterol gelators **1** and **2** were synthesized, and their gelation ability was evaluated in organic solvents. Very surprisingly, **1** + acetic acid gel results in spherical vesicles with two distinct sizes 200 and 2500 nm in diameter. In particular, the smaller vesicles are linked linearly, which is considered to serve as a driving-force for gelation. In contrast, **2** has a multilayered tubular structure. To characterize their aggregation modes in the gel phase, the organogels were observed by CD spectroscopy. The CD spectrum of **1** + acetic acid gel exhibits a negative sign for the first Cotton effect, indicating that the dipole moments in the gelator aggregate orient into an anticlockwise direction. On the other hand, **2** exhibits a positive sign for the first Cotton effect, indicating that they orient into a clockwise direction. The results indicate that the aggregate of **2** is stabilized by intermolecular cholesterol–cholesterol and azobenzene–azobenzene interactions, whereas the CD sign from the aggregate of **1** is indicative of an intramolecular azobenzene–azobenzene interaction. The spherical vesicle structures of organogel **1** were successfully transcribed into silica structures by the sol–gel polymerization of tetraethoxysilane (TEOS) in the gel phase. The TEM observation established that the wall of the spherical silica obtained in the acidic conditions consists of the multilayered vesicle structure. On the other hand, addition of Pd(NO₃)₂ changed the silica structure into fluffy globules with ~6000 nm in diameter. The EPMA observation established that Pd(II) ions are densely deposited on the surface of this globular silica. Hence, this process is useful as a new method to create metal catalytic sites on the silica support. These results indicate that the spherical multilayered structure of the organogel can be precisely transcribed into the silica structure. We thus believe that the sol–gel polymerization using molecular assembly templates strongly built in the organogel phase is a new strategy to create superstructured silica materials.

Introduction

Gelation of organic solvents by low-molecular weight compounds is the subject of increasing attention, not only because of numerous applications of the organogels to industrial purposes (e.g., in foods, deodorants, cosmetics, athletic shoes, and chromatography)¹ but in particular because of their striking properties to create various superstructures with respect to self-assembly phenomena.^{1–10} Fibrous aggregates of low-molecular

weight compounds formed by noncovalent interactions are responsible for such gelation phenomena. Hence, the xerogels can exhibit various superstructures, reflecting the monomeric structure of each gelator. This is why the organogel studies are considered to be a new field of supramolecular chemistry. More recently, it was found that certain cholesterol derivatives can gelate even tetraethoxysilane (TEOS), which results in silica by the sol–gel polymerization.¹¹ Very interestingly, it was shown that the sol–gel polymerization of gelated TEOS solutions affords novel silica with hollow lamellar,^{11a,b} helical,^{11c} or linear fiber^{11c,d} structures because the superstructures act as a template to create an inner tube during the TEOS polymeri-

* To whom correspondence should be addressed. E-mail: seijitcm@mbox.nc.kyushu-u.ac.jp.

(1) (a) Esch, J. V.; Schoonbeek, F.; Loos, M. d.; Kooijman, H.; Spek, A. L.; Kellogg, R. M.; Feringa, B. L. *Chem. Eur. J.* **1999**, *5*, 937. (b) Lu, I.; Cocker, T. M.; Bachman, R. E.; Weiss, R. G. *Langmuir* **2000**, *16*, 20. (c) Adballah, D. J.; Weiss, R. G. *Langmuir* **2000**, *16*, 352.

(2) Yoza, K.; Amanokura, N.; Ono, Y.; Akao, T.; Shinmori, H.; Takeuchi, M.; Shinkai, S.; Reinhoudt, D. N. *Chem. Eur. J.* **1999**, *5*, 2722.

(3) (a) Vries, E. J. de.; Kellogg, R. M. *J. Chem. Soc., Chem. Commun.* **1993**, 238. (b) Loos, M. de; Esch, J. van; Stokroos, I.; Kellogg, R. M.; Feringa, B. L. *J. Am. Chem. Soc.* **1997**, *119*, 12675.

(4) (a) Wang, R.; Geiger, C.; Chen, L.; Swanson, B.; Whittern, D. G. *J. Am. Chem. Soc.* **2000**, *122*, 2399. (b) Geiger, C.; Stanesch, M.; Chen, L. H.; Whittern, D. G. *Langmuir* **1999**, *15*, 5. 2241.

(5) (a) Hanabusa, K.; Okui, K.; Karki, K.; Koyama, T.; Shirai, H. *J. Chem. Soc. Chem. Commun.* **1992**, 1371. (b) Hanabusa, K.; Kawakami, K.; Kimura, M.; Shirai, H. *Chem. Lett.* **1997**, 191 and references therein.

(6) Sohna, J.-E. S.; Fages, F. *Chem. Commun.* **1997**, 327.

(7) (a) Otsuni, E.; Kamaras, P.; Weiss, R. G. *Angew. Chem., Int. Ed. Engl.* **1996**, *35*, 1324 and references therein. (b) Terech, P.; Furman, I.; Weiss, R. G. *J. Phys. Chem.* **1995**, *99*, 9558 and references therein.

(8) (a) Murata, K.; Aoki, M.; Suzuki, T.; Harada, T.; Kawabata, H.; Komori, T.; Ohseto, F.; Ueda, K.; Shinkai, S. *J. Am. Chem. Soc.* **1994**, *116*, 6664 and references therein. (b) James, T. D.; Murata, K.; Harada, T.; Ueda, K.; Shinkai, S. *Chem. Lett.* **1994**, 273. (c) Jeong, S. W.; Murata, K.; Shinkai, S. *Supramol. Sci.* **1996**, *3*, 83.

(9) Brotin, T.; Utermöhlen, R.; Fages, F.; Bouas-Laurent, H.; Desvergne, J.-P. *J. Chem. Soc., Chem. Commun.* **1991**, 416.

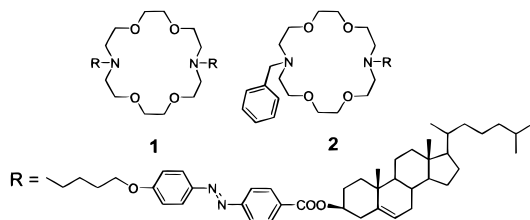
(10) (a) For recent comprehensive reviews, see Terech, P.; Weiss, R. G. *Chem. Rev.* **1997**, *97*, 3133. (b) Shinkai, S.; Murata, K. *J. Mater. Chem. (Feature Article)* **1998**, *8*, 485.

(11) (a) Jung, J. H.; Ono, Y.; Shinkai, S. *Langmuir* **2000**, *16*, 1643. (b) Jung, J. H.; Ono, Y.; Shinkai, S. *J. Chem. Soc., Perkin Trans 2* **1999**, 1289. (c) Ono, Y.; Nakashima, K.; Sano, M.; Kanekiyo, Y.; Inoue, K.; Hojo, J.; Shinkai, S. *Chem. Commun.* **1998**, 1477. (d) Ono, Y.; Kanekiyo, Y.; Inoue, K.; Hojo, J.; Shinkai, S. *Chem. Lett.* **1999**, 23. (e) Ono, Y.; Nakashima, K.; Sano, M.; Hojo, J.; Shinkai, S. *Chem. Lett.* **1999**, 1119.

zation process. One may thus consider that the unique superstructures in the organogels can be transcribed into the various silica structures: this means that the superstructures of organic aggregates, temporarily formed by noncovalent interactions, can be permanently fixed in inorganic materials.

Gokel et al. and others found that certain azacrown-appended cholesterol derivatives can form unique vesicular or lamellar structures in the absence and the presence of metal salts in aqueous solution.¹² They possess a polar azacrown headgroup and a suitable hydrophobic group to form stable aggregates, and the aggregate morphology can be adjusted by the ring size of the azacrown headgroup or the length of the hydrophobic group. It thus occurred to us that these superstructures created from the azacrown-appended cholesterol derivatives might be useful as a template for the transcription into the silica structure.

Mesoporous inorganic materials with vesicular structures have received special attention because of their potential applications as sorption media, molecular sieves, and catalysts.^{13,14} However, all of vesicular (multilayered) mesostructures reported to date had shells of undesirable thickness and shape. Recently, Pinnavaia and co-workers reported that arrangements of mesoporous inorganic materials with vesicular structures which showed 3–70 nm of thin shells have been accomplished by a “gemini”-type surfactants as template in aqueous solution.¹⁴ However, these particles have shells that consist of uni- and multi-lamellae.



We therefore designed gelator **1** which has two cholesterol and azobenzene moieties as the aggregate-forming sites and one azacrown moiety as a polar headgroup. We also prepared the gelator **2** as a reference for **1**. We have found that **1** not only gels various organic solvents but also acts as a template in the presence of metal salts or acidic medium for the sol–gel polymerization of TEOS to produce novel spherical structures of the silica. Here, we report a direct and highly efficient method toward the creation of novel spherical mesoporous silica with very thin shells (~ 5 – 20 nm) and ~ 200 – 2500 nm diameter by the sol–gel polymerization in the organogel phase. To the best of our knowledge, this is the first example not only for the multilayered spherical structure in the organogel system but also for the direct transcription of the molecular assemblies into the sphere of the silica in the organogel phase.

Results and Discussion

Characterization of Organogel Superstructures by Circular Dichroism (CD). The gelation ability was estimated for

(12) (a) Echegoyen, L. E.; Hernandez, J.; Kaifer, A. E.; Gokel, G. W.; Echegoyen, L. *J. Chem. Soc. Chem. Commun.* **1988**, 836. (b) Nakano, A.; Hernandez, J. C.; Dewall, S. L.; Wang, K.; Berger, D. R.; Gokel, G. W. *Supramol. Sci.* **1997**, *8*, 21. (c) Echegoyen, L. E.; Portugal, L.; Miller, S. R.; Hernandez, J. C.; Echegoyen, L.; Gokel, G. W. *Tetrahedron Lett.* **1988**, *29*, 4065. (d) Okahara, M.; Kuo, P. L.; Yamamura, S.; Ikeda, I. *J. Chem. Soc. Chem. Commun.* **1980**, 586.

(13) (a) Schacht, S.; Huo, Q.; Voigt-Martin, I. G.; Stucky, G. D.; Schüth, F. *Science* **1996**, *273*, 768. (b) Huo, Q.; Feng, J.; Schüth, F.; Stucky, G. D. *Chem. Mater.* **1997**, *14*, 119. (c) Caruso, F. *Chem. Eur. J.* **2000**, *6*, 413. (d) Caruso, F.; Caruso, R. A.; Möhwald, H. *Science* **1998**, *282*, 1111.

(14) (a) Tanev, P. T.; Ling, Y.; Pinnavaia, J. *Am. Chem. Soc.* **1997**, *119*, 8616. (b) Kim, S. S.; Zhang, W.; Pinnavaia, T. J. *Science* **1998**, *282*, 1302.

Table 1. Gelation Ability^a of **1** and **2** in Organic Solvents

entry	solvent	1	2	entry	solvent	1	2
1	chloroform	S	S	9	1-decanol	G	G
2	benzene	S	S	10	(<i>S</i>)-phenylethylamine	G	S
3	acetonitrile	I	I	11	(<i>R</i>)-phenylethylamine	G	S
4	DMSO	I	G	12	(<i>S</i>)-diaminocyclohexane	G	S
5	1-butanol	I	G	13	(<i>R</i>)-diaminocyclohexane	G	S
6	1-hexanol	G	G	14	pyridine	G	S
7	1-octanol	G	G	15	acetic acid	PG	S
8	1-nonanol	G	G	16	aniline	G	S

^a Gelator = 5.0 wt %; G: stable gel formed at room temperature; S: soluble; I: insoluble; PG: partially gelatinized.

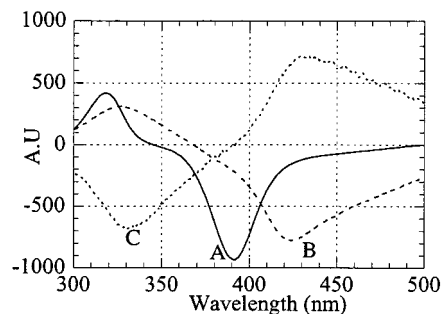


Figure 1. CD spectra of (A) **1** + acetic acid gel, (B) **1**•Pd(NO₃)₂ + aniline gel, and (C) **2** + cyclohexane gel.

16 different organic solvents containing **1** or **2**. As summarized in Table 1, **1** can gelate 11 out of 16 solvents, indicating that it acts as a versatile gelator of organic solvents. In particular, it is seen from Table 1 that the gelation ability for long-chain alcohols and amines is excellent. On the other hand, **2** can gelate only 6 out of 16 solvents. The difference suggests that the “gemini”-type cholesterol gelator is superior to conventional “mono”-type cholesterol gelator.

To characterize the aggregation mode in the organogel systems, CD (circular dichroism) spectra of the organogels were measured for **1** + acetic acid gel, **1**•Pd(NO₃)₂ + aniline gel, and **2** + butanol gel (Figure 1). In their CD spectra, the $\lambda_{\theta=0}$ values appear at 345 nm (absorption spectrum: $\lambda_{\max}=345$ nm), 368 nm (absorption spectrum: $\lambda_{\max}=368$ nm), and 390 nm (absorption spectrum: $\lambda_{\max}=375$ nm), respectively. One can thus assign these CD spectra to the exciton-coupling bands. It is known that azobenzene-appended cholesterol gelators with natural (S) C-3 configuration tend to give a positive sign for the first Cotton effect, indicating that the dipole moments of the azobenzene chromophores tend to orient into the clockwise direction.^{8a} Gelator **2** bearing only one cholesterol moiety also exhibits a positive sign for the first Cotton effect. In contrast, the CD spectra of **1** + acetic acid gel and **1**•Pd(NO₃)₂ + aniline gel exhibit a negative sign for the first Cotton effect, indicating that the dipole moments of the azobenzene chromophores orient into the anticlockwise direction. The CD maximum of **1** + acetic acid gel appears at shorter wavelength than that of **1**•Pd(NO₃)₂ + aniline gel, indicating that **1** in acetic acid can form the more stable gel than that of **1** + aniline gel in the presence of Pd(NO₃)₂. This shift in CD and UV can be explained by a better stacking of the azobenzene moieties.^{16c} In all cases, it was

(15) The xerogel more suitable to the SEM observation was obtained from cyclohexane solution (mp: 6.47 °C) than from a 1-butanol solution (mp: -90 °C), because this was prepared by a freezing-and-pumping method. The structure of xerogel does not depend on organic solvent according to ref 11.

(16) (a) Kunitake, T. *Angew. Chem., Int. Ed. Engl.* **1992**, *21*, 709. (b) Kunitake, T.; Ishikawa, Y.; Shimomura, M. *J. Am. Chem. Soc.* **1986**, *108*, 327. (c) Fuhrhop, J.-H.; Köning, J. *Membranes and Molecular Assemblies: The Synergetic Approach*; The Royal Society of Chemistry: 1994.

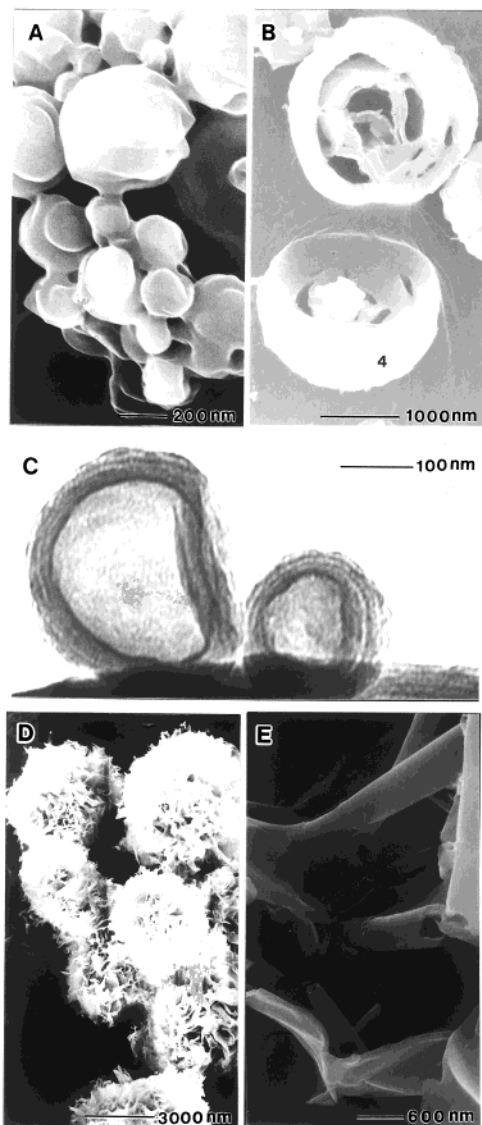


Figure 2. (A and B) SEM micrographs of the xerogel **1** prepared from acetic acid; (C) TEM micrograph of the xerogel **1** obtained from acetic acid (negatively stained by UO_2^{2+}), (D) SEM micrograph of the xerogel **1**·Pd(NO₃)₂ prepared from the aniline gel, and (E) SEM micrograph of the xerogel **2** prepared from the cyclohexane gel.

confirmed that the contribution of linear dichroism (LD) to the true CD spectra is negligible. These CD data support the view that the aggregation mode of **1** is somewhat different from that of **2**. It is undoubted that the organogels of **2** are formed by both intermolecular cholesterol–cholesterol and azobenzene–azobenzene interactions using the former interaction in the central columnar aggregate and the latter interaction in the side chain aggregate around the central column.^{8a} On the other hand, **1** in the organogels may adopt a folded conformation to enjoy efficient intramolecular cholesterol–cholesterol and azobenzene–azobenzene interaction, which may be the origin of the negative sign for the first Cotton effect. This problem will be discussed later in more detail.

Vesicular Structure of Organogels as Observed by SEM and TEM. To visually observe the aggregation modes in the organogel systems, the xerogels of **1** + acetic acid gel, **1**·Pd(NO₃)₂ + aniline gel, and **2** + cyclohexane gel were prepared by a freezing-and-pumping method from their gel phases below the sol–gel phase transition temperature and their SEM and TEM pictures were taken (Figure 2). The xerogel obtained from

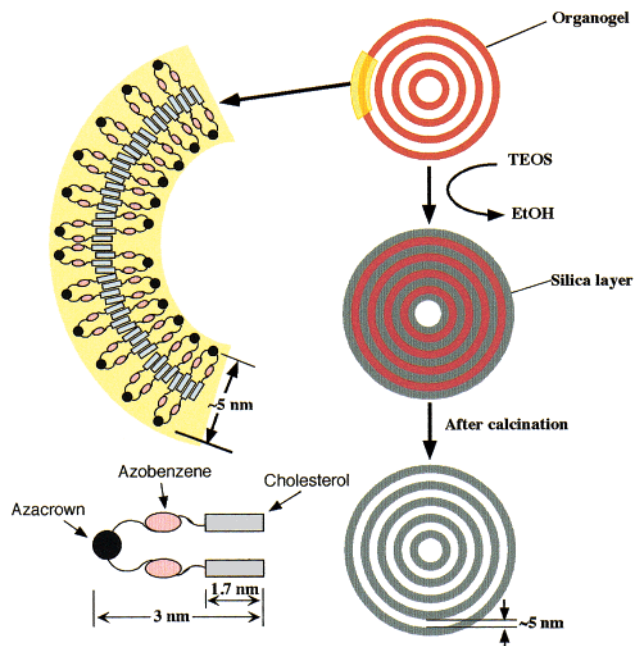


Figure 3. Schematic representation of sol–gel transcription of the multilayered spherical structure of the organogel **1**.

2 + cyclohexane gel shows the rolled film-like structure (Figure 2E), which is occasionally observed for less stable, inferior organogels.^{11,15} Very surprisingly, **1** + acetic acid gel results in two different spherical structures, one with ~200 nm diameter and the other with ~2500 nm diameter (Figure 2A and B: the overview picture supporting this explanation is shown in Supporting Information). The spherical morphology makes a sharp contrast from more common forms of organogels, fibrous or platelike. Further interesting is the finding that the smaller vesicles are connected to one another like a pearl necklace. Thus far, it has been believed that the fibrous aggregates are indispensable to gelation. Presumably, this new class of cross-link in the present system can be also the origin of the gelation phenomena. When **1** + acetic acid gel was dissolved by heating and sonicated by a 35 W tip sonicator for 15 min, the resultant SEM picture shows the increase in the concentration of the larger vesicle. One particle was cut by ultramicrotome (Figure 2B). It is seen from Figure 2B that the particle has the shell wall of ~2000 nm thickness and inner sphere of ~1000 nm. The clearer image of the larger vesicle was obtained from the TEM pictures. The **1** + acetic acid gel was translucent even in the presence of uranyl acetate, which was subjected to the TEM observation. The TEM picture (Figure 2C) clearly established that the shell wall consists of the multilayered structure with ~5 nm layer thickness and 200~350 nm diameter. In **1**, the solvophilic azacrown moiety and the solvophobic cholesterol moieties should occupy the surface and the inner part of the layer, respectively. Hence, the layer thickness of ~5 nm is commensurate with the vesicle wall structure as illustrated in Figure 3: that is, **1** adopts a folded conformation in which the cholesterol–cholesterol interaction occurs in the inner part in an interdigitated manner and the azobenzene–azobenzene interaction occurs primarily in an intramolecular manner and second in an intermolecular manner toward the lateral direction. This aggregation mode is compatible with the ~5 nm layer thickness and well explains the reason the CD spectra are different from those of **2** which features the one-dimensional molecular stacking^{8a} (Figure 1). To the best of our knowledge, this is the first example for the creation of multilayered spherical vesicles in organic media (acetic acid for **1**). This system is quite

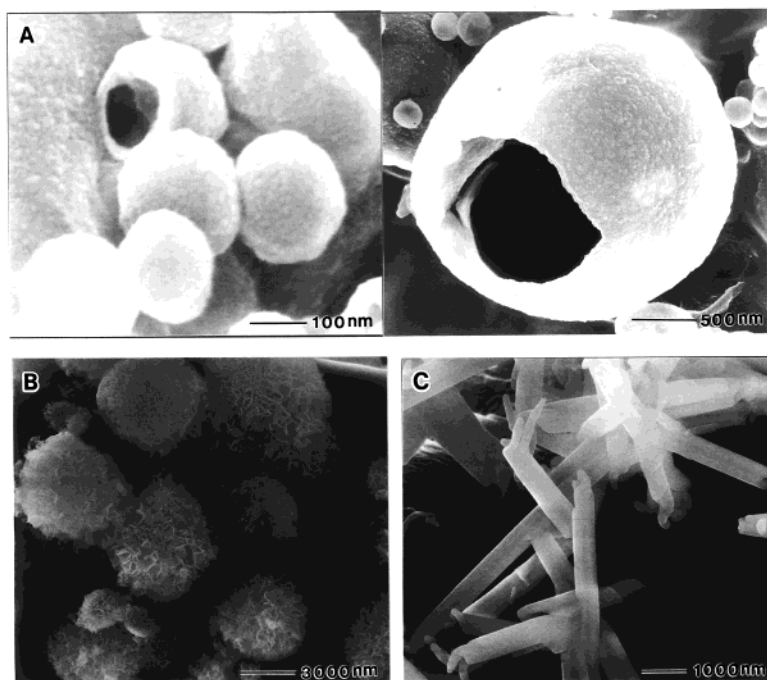


Figure 4. SEM micrographs of the silica obtained from (A) **1** + acetic acid gel, (B) **1**•Pd(NO₃)₂ + aniline gel, and (C) **2** + acetic acid gel.

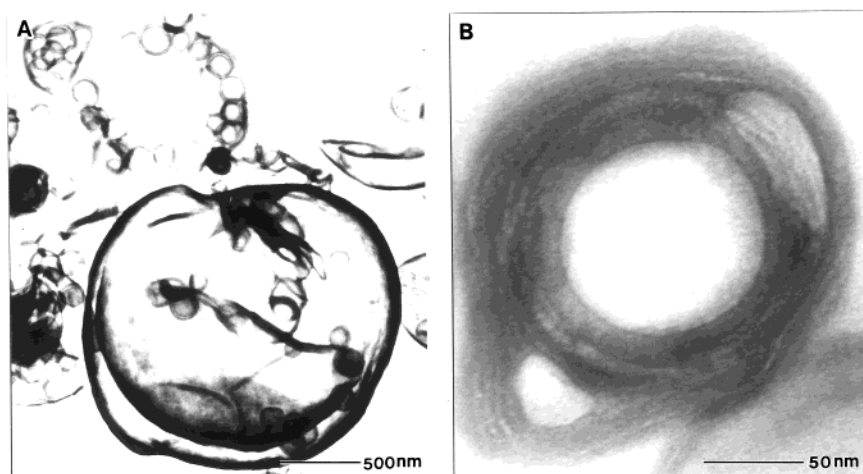


Figure 5. TEM micrographs of the silica obtained from **1** + acetic acid gel (A) before and (B) after sectioning.

different from azacrown-appended cholesterol surfactants previously reported by Gokel et al. which have long methylene groups between the azacrown headgroup and the cholesterol group.^{12a-c} This surfactant can only form vesicular and lamellar structures in aqueous solution, whereas **1** can form the vesicular structure even in organic solvents. In addition, Kunitake and co-workers have reported on a bilayer assembly of azobenzene amphiphiles containing a cyclic tetramine group as a hydrophilic head. Since they only form rodlike aggregates with 3–4 nm diameters and several hundred to 200 nm lengths in aqueous solution,¹⁶ the present system is also different from Kunitake's system.

Sol–Gel Polymerization of TEOS and SEM/TEM Observation of Silica Structures. To transcribe these novel superstructures constructed in the organogels to silica, sol–gel polymerization of TEOS was carried out in the gel phase of **1** and **2** at room temperature for 7 days.¹¹ One may expect that oligomeric silica species with the anionic charge interact with protonated azacrown moieties with the cationic charge and the multilayered vesicular structure is successfully transcribed into the silica structure (as illustrated in Figure 3). Figure 4 shows the SEM micrographs of the silica taken after calcination. From

1 + acetic acid gel, the spherical silica structures are yielded (Figure 4A). As expected, one can observe both the cross-linked smaller particles with ~200 nm diameter and the isolated larger particles with ~2500 nm in diameter. Figure 4A accidentally catches one broken particle (the enlarged particle is shown in the right). It is seen from these images that the inside of these particles have cavity inside. Presumably, this breakage is induced by vacuum necessary to the SEM sample preparation.

To further corroborate that the spherical structure of the organogel really acted as a template for the creation of the spherical silica, we took TEM pictures after removal of **1** by calcination. Figure 5A reveals that both the smaller and the larger spherical particles have a hollow structure. After sectioned with a ultramicrotome, the edge of the small particle was observed with TEM (Figure 5B). It is seen from this TEM image that the shell wall consists of the multilayered lamella having 5 nm spacing.¹⁷ These results clearly support the view that the multilayered structure of the organogels is precisely transcribed into the silica structure. We believe that such a precise transcription becomes possible for the first time by using the

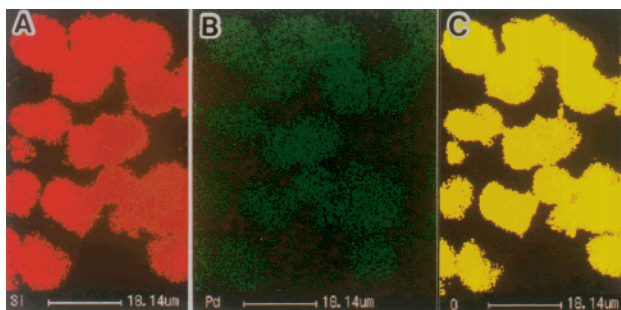


Figure 6. EPMA pictures of the silica obtained from $1 \cdot \text{Pd}(\text{NO}_3)_2 +$ aniline gel: (A) silicon map, (B) palladium map, and (C) oxygen map.

organogel superstructures as a template which have the crystal-like characters.^{8,10,11}

In contrast, the silica obtained from the acetic acid gel of **2** features the roll-paperlike tubular structure with 450–500 nm outer diameter and 150–170 nm inner diameter (Figure 4C). It is known that this structure results from the sol–gel polymerization of TEOS along the curved films of **2** (Figure 2E).^{11a}

Deposition of Palladium Particle on Silica Surface by Host–Guest Interaction. It is known that azacrown ethers have a high affinity with metal cations. When sol–gel polymerization of TEOS is carried out around the metal-binding organogel superstructures, the metals would be deposited on the surface of the silica after calcination. With this intriguing idea in mind, we added $\text{Pd}(\text{NO}_3)_2$ to the organogel system. Although many organic solutions containing **1** and $\text{Pd}(\text{NO}_3)_2$ could not be gelled, we eventually found that the aniline solution is sufficiently gelled. A SEM picture of the xerogel obtained from the aniline solution is shown in Figure 2D. The vesicular structure is no longer observable: instead, the fluffy globular aggregates with ~ 6000 nm diameter appear. Careful examination of the aggregates reveals that the surface consists of the canna-flower-like coating with ~ 50 nm thickness. The results indicate that Pd(II) ions bound to the surface azacrown drastically change the morphology.

As the preliminary step toward the design of the metal-deposited silica for catalytic application,¹⁸ we carried out the sol–gel polymerization in $1 \cdot \text{Pd}(\text{NO}_3)_2 +$ aniline gel. It is seen from Figure 4B that the silica structure which is very similar to that of the xerogel (Figure 2D) results. The metal deposition on the silica is usually detectable by the TEM observation,^{11b} but in the present sample the silica particles were too thick to obtain the clear TEM picture. We thus estimated the Pd content by X-ray electron probe microanalyzer (EPMA). Figure 6 clearly shows that Pd(0) and Pd(II) are deposited on the silica surface, the content being 1.8 wt %.¹⁹ The results indicate that the azacrown-containing gelator is useful as a new metal-deposition method on the silica matrix.

Conclusions

The present study has demonstrated that azacrown-appended cholesterol gelator **1** creates the novel multilayered spherical

(17) In fact, we have already measured XRD. The peak which deserves publication was not observed, however. Judging from the TEM pictures, the space between silica layers is about 5 nm. One should note that this is the “averaged” value and there is a significant distribution in the spacing. We thus consider that this distribution is the reason we could not observe the peak in XRD. The many reproducible TEM pictures support, however, that there exist a clear space between the silica.

(18) (a) Mehnert, C. P.; Weaver, D. W.; Ying, J. Y. *J. Am. Chem. Soc.* **1998**, *120*, 12289. (b) Mehnert, C. P.; Ying, J. Y. *Chem. Comm.* **1997**, 2215.

(19) Chemical component of Pd was confirmed by Electron Spectroscopy for Chemical Analysis (ESCA): it consists of Pd(0) and Pd(II) derivative.

structure in acetic acid, whereas **1** results in the fluffy globular aggregates in the presence of $\text{Pd}(\text{NO}_3)_2$. In contrast, **2** shows the tubular lamellar structure. Sol–gel polymerization of TEOS in the presence of the multilayered spherical structure of **1** and the lamellar aggregates of **2** is useful to create the multilayered spherical and the tubular structure of the silica, respectively. The Pd particles are deposited on the surface of the silica by host–guest interaction.

In general, organic materials are capable of construction of a variety of supramolecular structures reflecting their own molecular shape, whereas such “shape design” is very difficult from inorganic materials. The present findings suggest, as also suggested by a few other research groups, that various novel assembly structures created by weak intermolecular forces can be imprinted as permanent structures in inorganic materials. The present study clearly demonstrates that the organogel system is one of the most suitable molecular assemblies for this transcription. We believe, however, that the present silica with the unique higher-order morphology is still very useful for drug delivery, nanosized microcapsulation, compartmentalization, etc.

Experimental Section

Apparatus for Spectroscopy Measurement. ^1H and ^{13}C NMR spectra were measured on a Bruker ARX 300 apparatus. IR spectra were obtained in KBr pellets using a Shimadzu FT-IR 8100 spectrometer, and MS spectra were obtained by a Hitachi M-250 mass spectrometer.

TEM Observation. Samples for transmission electron microscope (TEM) studies were embedded in White acrylic resin (hard) and sectioned on an ultramicrotome. The thin sections (~ 20 nm) were supported on the 400 mesh copper grids. Transmission electron microscopy was done with a Hitachi H-7100, using accelerating voltage of 100 kV and a 16 mm working distance. Multilayered structure of the organogel was attached to Butvar/carbon-coated, 400 mesh copper grids by applying 10–15 μL drops of the organogel solution containing to 15 μL of uranyl acetate onto the grids and allowing them to remain for 1–5 min. Excess fluid was wiped off the grids by touching their edges by filter paper.

SEM Observation. Scanning electron microscopy (SEM) was done with a Hitachi S-4500. The thin gel was prepared in a 1–2 mL bottle and frozen in liquid nitrogen or dry ice–acetone. The frozen specimen was evaporated by a vacuum pump for 24 h. The dry sample was coated by palladium–platinum. The accelerating voltage of SEM was 5–15 kV, and the emission current was 10 μA .

Gelation Test of Organic Fluids. The gelator and the solvent were put in a septum-capped test tube and heated in an oil bath until the solid was dissolved. The solution was cooled at room temperature. If the stable gel was observed at this stage, it was classified as G in Table 1.

Sol–Gel Polymerization of TEOS. In a typical preparation a 5.8×10^{-6} M quantity of gelator in the absence and the presence of metal salt (5.8×10^{-6} M) were dissolved in 1.0 g of tetrahydrofuran. The solution was evaporated to dryness. The residual solid was added to acetic acid or aniline (95 mg)/TEOS (15.0 mg)/water (5.7 mg)/benzylamine (5.6 mg) and warmed until a transparent solution was obtained. The reaction mixture was placed at room temperature under the static conditions for 7 days. The product was dried by a vacuum pump at room temperature. Finally, the gelator was removed by calcination at 200 $^\circ\text{C}$ for 2 h and 500 $^\circ\text{C}$ for 2 h under a nitrogen atmosphere and 500 $^\circ\text{C}$ for 4 h under aerobic conditions.

4-*N*-Monobromobutoxyl-4'-((cholesteryloxy)carbonyl)azobenzene (4). 4-((Bromo-butylxyphenyl)azo)benzoic acid **3** (0.7 g, 1.86 mmol) and cholesterol (0.718 g, 2.23 mmol) were dissolved in 20 mL of dichloromethane under a nitrogen atmosphere. The solution was maintained at 0 $^\circ\text{C}$ with an ice bath. The dicyclohexylcarbodiimide (DCC) (0.383 g, 1.86 mmol) and (dimethylamino)pyridine (DMAP) (0.022 g, 0.186 mmol) were then added, the reaction mixture being stirred for 4 h at 0 $^\circ\text{C}$. The reaction mixture was filtered, and the filtrate

was washed with acidic and basic aqueous solutions (50 mL each). The organic layer was evaporated to dryness. The residue was purified by a silica gel column eluting with THF/*n*-hexane (1:6 v/v) to give compound **4** in yield 26% as yellow solid (mp = 141.5 °C). ¹H NMR (300 MHz, CDCl₃) δ (ppm) = 8.17 (2H, d, *J* = 9.0 Hz), 7.72 (2H, d, *J* = 9.0 Hz), 7.90 (2H, d, *J* = 9.0 Hz), 7.10 (2H, d, *J* = 9.0 Hz), 5.45 (1H, d, *J* = 6.3 Hz), 5.02–4.88 (1H, m), 4.1 (2H, t, *J* = 6.3 Hz), 3.52 (2H, t, *J* = 6.2 Hz), 2.49 (2H, d, *J* = 6.2 Hz), 2.28–0.94 (35H, m), 0.88 (3H, s). ¹³C NMR (75 MHz, CDCl₃) δ (ppm) = 165.1, 161.88, 155.20, 146.98, 139.9, 130.2, 125.18, 122.84, 122.28, 114.72, 67.22, 66.67, 56.67, 56.11, 50.01, 42.30, 39.71, 39.50, 38.20, 37.01, 36.64, 36.17, 35.79, 33.32, 31.92, 31.86, 29.3, 28.32, 28.01, 27.88, 27.78, 24.28, 23.82, 22.83, 22.56, 21.04, 19.38, 19.38, 18.71, 11.86. MS(SIMS) = 745 [M + H]⁺. IR (KBr) 3005, 1722, 1603, 1579, 1500, 1468, 1284, 1116, 1047 cm⁻¹.

4-(*N*-Monobenzylaza-18-crown-6-butoxy)-4'-(cholesteyloxy)carbonyl)azo- benzene (2). A mixture of compound **4** (0.13 g, 0.174 mmol), monobenzyl diaza-18-crown-6 (0.061 g, 0.1740 mmol), and sodium carbonate (0.784 g, 1.74 mmol) in dry butyronitrile (15 mL) was refluxed for 24 h. The solution was filtered after cooling, the filtrate being concentrated to dryness by a vacuum evaporator. The residue was purified by an aluminum oxide column with ethanol/dichloromethane (1:30 v/v) to give the desired product in yield 75.8% as a yellow solid (mp = 113.3–115.2 °C). ¹H NMR (300 MHz, CDCl₃) δ (ppm) = 8.17 (2H, d, *J* = 9.1 Hz), 7.93 (2H, d, *J* = 9.1 Hz), 7.31–7.26 (7H, m), 6.95 (2H, d, *J* = 9.0 Hz), 5.45 (1H, d, *J* = 6.5 Hz), 4.90 (1H, m), 4.08 (2H, t, *J* = 6.5 Hz), 3.73–3.61 (32H, m), 2.78 (4H, t, *J* = 12.1 Hz), 2.75 (2H, t, *J* = 6.5 Hz), 2.49 (2H, d, *J* = 6.3 Hz), 2.01–0.69 (35H, m). ¹³C NMR (75 MHz, CDCl₃) δ (ppm) = 165.47, 162.13, 155.19, 146.80, 139.54, 134.77, 130.48, 125.13, 122.79, 122.22, 114.72, 74.79, 70.84, 70.73, 70.70, 70.35, 68.14, 56.62, 56.06, 53.94, 49.87, 42.25, 39.66, 39.45, 38.16, 36.97, 36.60, 36.12, 35.75, 31.88, 28.19,

27.96, 27.84, 26.96, 24.24, 23.78, 22.79, 22.53, 21.00, 19.34, 18.67, 11.81. MS(SIMS) = 1019 [M + 2H]⁺. IR (KBr) 3010, 2943, 2868, 1711, 1595, 1585, 1500, 1463, 1417, 1404, 1275, 1140, 1109 cm⁻¹. Anal. Calcd for C₆₃H₉₂N₄O₇: C, 74.41; H, 9.12; N, 5.91. Found: C, 73.70; H, 9.12; N, 5.51.

4-(*N*-1,10-Diaza-18-crown-6-butoxy)-4'-(bis(cholesteyloxy)carbonyl)azobenzene (1). A mixture of compound **4** (0.25 g, 0.335 mmol), diaza-18-crown-6 (0.17 g, 0.67 mmol), and sodium carbonate (0.70 g, 6.7 mmol) in dry butyronitrile (35 mL) was refluxed for 48 h. The solution was filtered after cooling, the filtrate being concentrated to dryness by a vacuum evaporator. The residue was purified by an aluminum oxide column with ethanol/dichloromethane (1:50 v/v) to give the desired product in yield 50.5% as yellow solid (mp = 203.5–205.5 °C). ¹H NMR (300 MHz, CDCl₃) δ (ppm) = 8.17 (4H, d, *J* = 9.0 Hz), 7.93 (4H, d, *J* = 9.0 Hz), 7.88 (4H, d, *J* = 9.0 Hz), 6.97 (4H, d, *J* = 9.0 Hz), 5.45 (2H, d, *J* = 6.3 Hz), 4.87 (2H, m), 3.98 (4H, t, *J* = 6.3 Hz), 3.73–3.61 (26H, m), 2.83–2.80 (10H, m), 2.60 (4H, t, *J* = 6.2 Hz) 2.01–0.69 (82H, m). ¹³C NMR (75 MHz, CDCl₃) δ (ppm) = 165.67, 161.52, 155.35, 145.02, 137.54, 130.48, 123.13, 122.24, 114.72, 86.94, 70.84, 70.73, 68.53, 56.62, 55.35, 53.94, 49.22, 39.23, 38.16, 37.01, 36.97, 36.35, 36.25, 35.12, 31.35, 27.96, 27.35, 24.24, 23.78, 22.79, 22.53, 21.00, 19.34, 18.67, 11.86. MS (SIMS) = 1592 [M + H]⁺. IR (KBr) 3005, 2940, 1722, 1603, 1579, 1500, 1468, 1284, 1116, 1047 cm⁻¹. Anal. Calcd for C₁₀₀H₁₄₆N₆O₁₀: C, 75.43; H, 9.24; N, 5.28. Found: C, 75.26; H, 9.23; N, 5.17.

Supporting Information Available: An overview pictures of SEM for the xerogel **1** prepared from acetic acid (PDF). This material is available free of charge via the Internet at <http://pubs.acs.org>.

JA001623F